Mineralogical Magazine (2022), **86**, 436–446
doi:10.1180/mgm.2022.36

CAMBRIDGE UNIVERSITY PRESS

Article

Goldhillite, $Cu_5Zn(AsO_4)_2(OH)_6{\cdot}H_2O$, a new mineral species, and redefinition of philipsburgite, $Cu_5Zn[(AsO_4)(PO_4)](OH)_6{\cdot}H_2O$, as an As–P ordered species

Rezeda M. Ismagilova[1*], Branko Rieck[2], Anthony R. Kampf[3], Gerald Giester[2], Elena S. Zhitova[1,4], Christian L. Lengauer[2], Sergey V. Krivovichev[1,5], Andrey A. Zolotarev[1], Justyna Ciesielczuk[6], Julia A. Mikhailova[7], Dmitry I. Belakovsky[8], Vladimir N. Bocharov[1], Vladimir V. Shilovskikh[1], Natalia S. Vlasenko[1], Barbara P. Nash[9] and Paul M. Adams[3]

[1]St. Petersburg State University, Universitetskaya nab. 7/9, St. Petersburg 199034, Russia; [2]Institut für Mineralogie und Kristallographie, Universität Wien, Althanstraße 14, 1090, Austria; [3]Natural History Museum of Los Angeles County, 900 Exposition Blvd., Los Angeles, CA 90007, United States of America; [4]Institute of Volcanology and Seismology, Russian Academy of Sciences, Boulevard Piip 9, Petropavlovsk-Kamchatsky 683006, Russia; [5]Nanomaterials Research Centre, Kola Science Centre, Russian Academy of Sciences, Fersman Street 14, Apatity 184209, Russia; [6]Faculty of Earth Sciences, University of Silesia, Będzińska 60, 41–200 Sosnowiec, Poland; [7]Geological Institute, Kola Science Centre, Russian Academy of Sciences, Fersman Street 14, Apatity 184209, Russia; [8]Fersman Mineralogical Museum, Russian Academy of Sciences, Leninsky Prospekt 18-2, Moscow 119071, Russia; and [9]Department of Geology and Geophysics, University of Utah, Salt Lake City, UT 84112, United States of America

Abstract

Philipsburgite has been redefined as the intermediate member of the goldhillite–philipsburgite–kipushite isomorphous series with the ideal formula $Cu_5Zn[(AsO_4)(PO_4)](OH)_6{\cdot}H_2O$ due to the site-selective As–P substitution. The new mineral goldhillite, ideally $Cu_5Zn(AsO_4)_2(OH)_6{\cdot}H_2O$ [or $Cu_5Zn(AsO_4)(AsO_4)(OH)_6{\cdot}H_2O$], is the arsenate end-member of this series. Goldhillite occurs on fracture surfaces in a rock comprised mostly of quartz with iron hydroxides in association with mixite, cornwallite and conichalcite. Goldhillite forms transparent, bright emerald-green, tabular crystals with vitreous lustre, flattened on {100}, up to 1 mm across and in rosettes up to 1.5 mm. The mineral is brittle with uneven fracture and perfect cleavage on {100}; the Mohs hardness is 3.5. The calculated density for the holotype is 4.199 g cm^{-3}. The Raman spectrum is consistent with the presence of H_2O-molecules, OH-groups, AsO_4 tetrahedra and traces of PO_4. Electron microprobe analyses of goldhillite (H_2O content based on the crystal structure) provided: CuO 48.91, ZnO 13.18, As_2O_5 26.06, P_2O_5 3.25, H_2O 8.97, total 100.37 wt.%. The empirical formula for goldhillite based on O = 15 apfu is $(Cu_{4.69}Zn_{1.23})_{\Sigma 5.92}(As_{0.86}P_{0.18}O_4)_2(OH)_{5.61}{\cdot}H_2O$. The crystal structures of goldhillite and philipsburgite were determined using single-crystal X-ray diffraction data and refined to $R_1 = 0.054$ (for 2365 $I > 2\sigma I$ reflections) and 0.052 (for 2308 $I > 2\sigma I$ reflections), respectively. Goldhillite is monoclinic, $P2_1/c$, $a = 12.3573(5)$, $b = 9.2325(3)$, $c = 10.7163(4)$ Å, $\beta = 97.346(4)°$, $V = 1212.59(8)$ Å^3 and $Z = 4$. Philipsburgite is monoclinic, $P2_1/c$, $a = 12.3095(9)$, $b = 9.2276(3)$, $c = 10.7195(3)$ Å, $\beta = 97.137(7)°$, $V = 1208.16(10)$ Å^3 and $Z = 4$. The strongest lines of the powder X-ray diffraction pattern of goldhillite [*d*, Å (*I*, %)(*hkl*)] are: 4.09 (28)(300), 3.41 (23)(12$\bar{2}$, 221, 311), 2.57 (100)(132, 11$\bar{4}$, 20$\bar{4}$), 2.17 (18)(42$\bar{3}$, 332), 1.95 (22)(432) and 1.54 (20)(13$\bar{6}$, 060). Goldhillite is named after its type locality, the Gold Hill mine, Tooele County, Utah, USA.

Keywords: goldhillite, new mineral, philipsburgite, kipushite, As–P ordering, crystal structure, Raman spectroscopy, Gold Hill mine, Black Pine mine, Kamariza mines, Silver Coin mine

(Received 22 December 2021; accepted 30 March 2022; Accepted Manuscript published online: 13 May 2022; Associate Editor: Juraj Majzlan)

Introduction

There are currently more than 110 copper arsenate minerals and more than 40 copper phosphate minerals; however, only three among them, epifanovite (Yakovenchuk *et al.*, 2017), milkovoite (Siidra *et al.*, 2021) and philipsburgite, have arsenate and phosphate dominating different structural sites.

Philipsburgite was originally described from the Black Pine mine, north of Philipsburg, Montana, USA, with the formula $(Cu,Zn)_6[(As,P)O_4]_2(OH)_6{\cdot}H_2O$ by Peacor *et al.* (1985), who concluded that philipsburgite is isotypic with kipushite, $Cu_5Zn(PO_4)_2(OH)_6{\cdot}H_2O$ (Piret *et al.*, 1985). They reported the empirical chemical formula $Cu_{4.30}Zn_{1.65}[(AsO_4)_{1.05}(PO_4)_{0.91}](OH)_{6.03}{\cdot}1.04H_2O$ and, based on the small predominance of As over P, defined philipsburgite as an As-dominant species.

***Author for correspondence:** Rezeda M. Ismagilova, Email: rezeda_marsovna@inbox.ru
Cite this article: Ismagilova R.M., Rieck B., Kampf A.R., Giester G., Zhitova E.S., Lengauer C.L., Krivovichev S.V., Zolotarev A.A., Ciesielczuk J., Mikhailova J.A., Belakovsky D.I., Bocharov V.N., Shilovskikh V.V., Vlasenko N.S., Nash B.P. and Adams P.M. (2022) Goldhillite, $Cu_5Zn(AsO_4)_2(OH)_6{\cdot}H_2O$, a new mineral species, and redefinition of philipsburgite, $Cu_5Zn[(AsO_4)(PO_4)](OH)_6{\cdot}H_2O$, as an As–P ordered species. *Mineralogical Magazine* **86**, 436–446. https://doi.org/10.1180/mgm.2022.36

The crystal structure study of 'philipsburgite' from the Middle Pit, Gold Hill mine, Tooele County, Utah, USA, with the empirical formula $Cu_{4.69}Zn_{1.23}[(AsO_4)_{1.72}(PO_4)_{0.36}](OH)_{5.61}\cdot H_2O$, reported by Krivovichev *et al.* (2018) revealed the existence of a site-selective As–P substitution for the two tetrahedral sites with the As1 site (designated as the *T*1 site herein) preferred for the incorporation of P and the As2 site (designated as the *T*2 site herein) preferred for the incorporation of As. The sample studied by Krivovichev *et al.* (2018) exhibits As >> P with both tetrahedral sites occupied predominantly by As.

New crystal-structure studies of philipsburgite from the Black Pine (holotype), the Silver Coin and Kamariza mines revealed the ordered distribution of P and As over *T*1 and *T*2 tetrahedral sites, leading to the conclusion that philipsburgite, defined previously with the formula $Cu_5Zn[(As,P)O_4]_2(OH)_6\cdot H_2O$, should be redefined with the formula $Cu_5Zn[(AsO_4)(PO_4)](OH)_6\cdot H_2O$, i.e. as a mineral characterised by an ordered distribution of As and P. At the same time, the 'philipsburgite' sample studied by Krivovichev *et al.* (2018) qualifies as a separate mineral species with the ideal formula $Cu_5Zn[(AsO_4)_2](OH)_6\cdot H_2O$ [or $Cu_5Zn(AsO_4)(AsO_4)(OH)_6\cdot H_2O$], i.e. as the As-analogue of kipushite, which has both *T*1 and *T*2 sites predominantly occupied by As. In addition, a sample from the Yamato Mine, Yamaguchi Prefecture, Japan, described by Shirose and Uehara (2011) as philipsburgite, is noted to have a composition corresponding most closely to the As end-member.

A common occurrence of goldhillite, philipsburgite and kipushite is known from the Sa Duchessa mine, Orrida, Domusnovas, Sardinia, Italy (Olmi *et al.*, 1988). The analysis of a slightly different material from the initial discovery of philipsburgite also revealed the existence of goldhillite at the Christiana mine No. 132, Kamariza mines, Greece (Supplementary Fig. S1) where philipsburgite was originally found. The empirical formula is $Cu_{4.97}Zn_{1.09}[(AsO_4)_{1.55}(PO_4)_{0.45}](OH)_6\cdot H_2O$ (P + As = 2 and O = 15 atoms per formula unit (apfu)) (B. Rieck, personal communication, October 5, 2021).

This paper describes the new mineral goldhillite as the As-dominant member of the kipushite–philipsburgite–goldhillite isomorphous series and redefines philipsburgite as an As–P-ordered intermediate species in that series, with kipushite remaining as the P-dominant member.

In the absence of structure refinement, members of the series with P:As > 3:1 can be identified as kipushite and those with As:P > 3:1 can be identified as goldhillite. Members with roughly equal amounts of P and As certainly qualify as philipsburgite; however, it is impossible to precisely specify compositional boundaries between kipushite and philipsburgite and between goldhillite and philipsburgite because the *T*1 and *T*2 may, at least theoretically, contain different amounts of P and As.

The new mineral and its name have been approved by the Commission on New Minerals, Nomenclature and Classification (CNMNC) of the International Mineralogical Association (IMA2021-034, Ismagilova *et al.*, 2021) and the redefinition of philipsburgite has been approved by the CNMNC (voting proposal 20-G, Miyawaki *et al.*, 2021). Goldhillite is named after its type locality, the Gold Hill mine, Tooele County, Utah, USA.

Materials

Philipsburgite crystals from the following occurrences were investigated: (1) the Black Pine mine, Philipsburg, Montana, USA (holotype specimen; U.S. National Museum of Natural History, Smithsonian Institution, #161201) (BP); (2) Christiana mine No. 132, Kamariza mines, Agios Konstantinos, Lavrion district mines, Lavreotiki, East Attica, Attica, Greece (KM) (Supplementary Fig. S2); and (3) the Silver Coin mine, Valmy, Iron Point district, Humboldt County, Nevada, USA (SC). The SC sample is stored under catalogue number 76195 in the Natural History Museum of Los Angeles County (Los Angeles, California, USA).

The description of goldhillite is based on the material from the Gold Hill mine, Tooele County, Utah, USA. The holotype is from the collection of the Fersman Mineralogical Museum (Moscow, Russia), where it is stored under catalogue number 88338 (FMM). The cotype is from the collection of the Natural History Museum of Los Angeles County (NHMLA), where it is stored under catalogue number 76142.

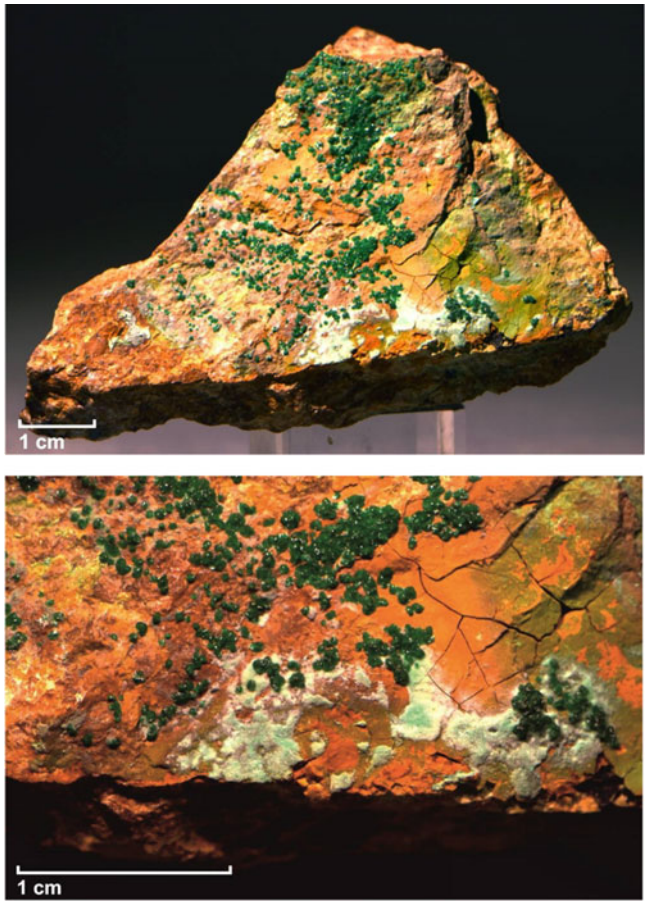

Fig. 1. Holotype specimen # 88338 from the collection of the Fersman Mineralogical Museum with emerald green crystals of goldhillite along with a pale greenish fine-grained aggregates and fine needles (up to 0.4 mm long) of zálesíite: FOV 6 × 8 cm (upper image), FOV 3 × 2 cm (lower image). Photo: M.M. Moiseev.

Experimental methods and data processing

Goldhillite

The FMM sample was referred to as 'philipsburgite' by Krivovichev *et al.* (2018). The study involved single-crystal X-ray diffraction at 100 K and electron microprobe analysis. In the present study, we report the Raman spectrum, powder X-ray diffraction data and optical data for the FMM sample, chemical data for the NHMLA

https://doi.org/10.1180/mgm.2022.36 Published online by Cambridge University Press

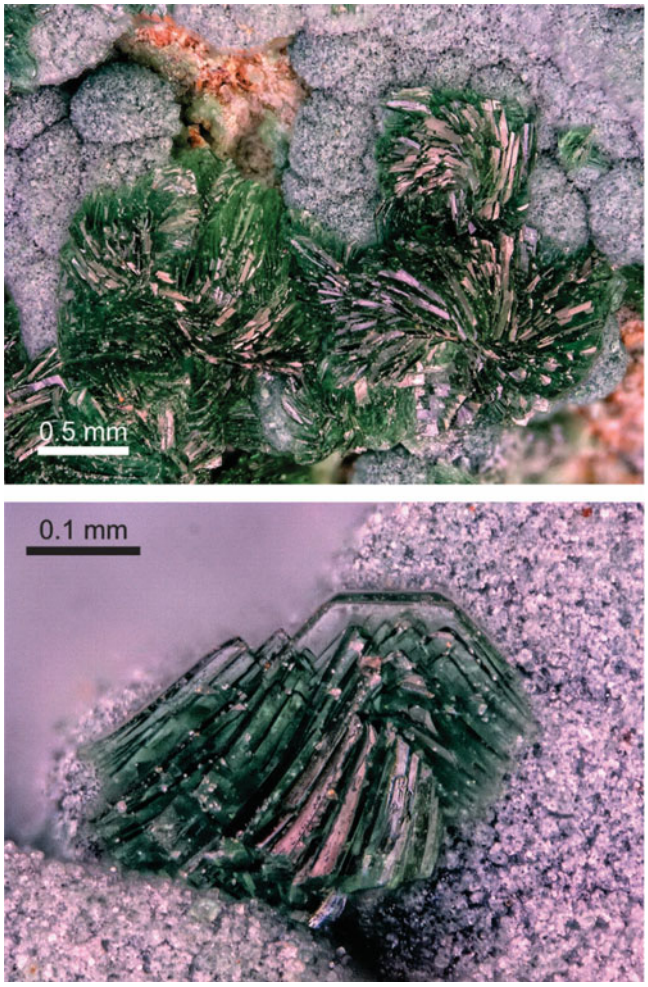

Fig. 2. Goldhillite on the cotype specimen (#76142) from the collection of the Natural History Museum of Los Angeles County with emerald green crystals of goldhillite on botryoidal cornwallite coated with tiny crystals of conichalcite.

sample and the room-temperature crystal structure study of FMM and NHMLA required for the complete description of a new mineral species.

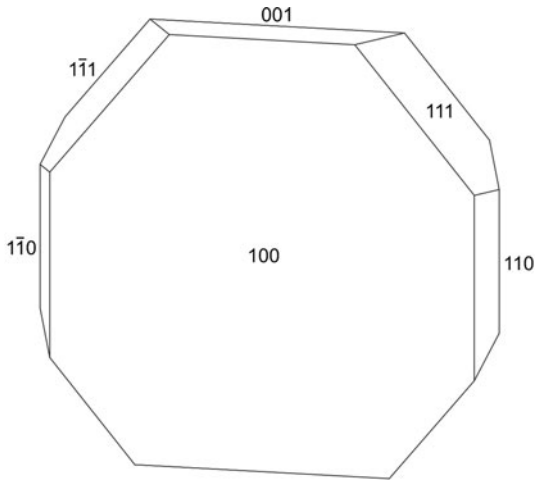

Fig. 3. Crystal drawing of goldhillite; clinographic projection.

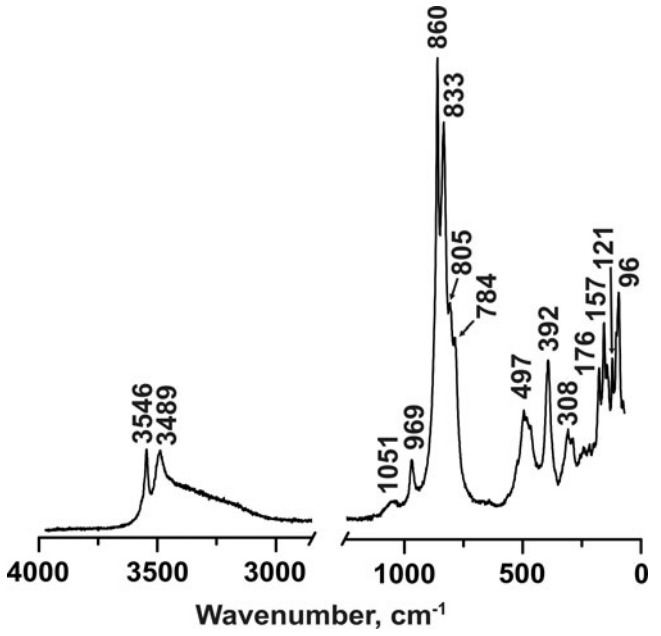

Fig. 4. Raman spectrum of goldhillite.

The Raman spectrum of FMM goldhillite was obtained by means of a Horiba Jobin-Yvon LabRam HR 800 spectrometer equipped with an Ar+ laser (λ = 514 nm) at ~6 mW power at the sample. The Raman spectrum was recorded at room temperature in the range from 70 to 4000 cm^{-1} with resolution of 2 cm^{-1} and processed using the *LabSpec* (Horiba Jobin Vyon, 2008) and *Origin* software (OriginLab Corporation, 2009).

Powder X-ray diffraction data for the FMM sample were collected on a Rigaku R-Axis Rapid II diffractometer (Debye-Scherrer geometry, d = 127.4 mm) equipped with a rotating anode X-ray source (Co*K*α, λ = 1.79021 Å) and a curved image plate detector. The data were integrated using the software package *Osc2Tab/SQRay* (Britvin *et al.*, 2017). Unit-cell parameters were refined using the Le Bail methods implemented in *TOPAS* software (Bruker-AXS, 2009).

Single-crystal X-ray diffraction studies of goldhillite samples were carried out using an Agilent Technologies Xcalibur Eos diffractometer (for the FMM sample) and a Rigaku R-Axis Rapid II curved imaging plate microdiffractometer (for the NHMLA sample) at room temperature (293 K). The data were collected using monochromatic Mo*K*α X-radiation at 50 kV and 40 mA. The structure data for FMM were integrated and corrected by means of the *CrysAlisPro* (Agilent Technologies, 2014) program package, which was also used for an empirical absorption correction using spherical harmonics, as implemented in the *SCALE3 ABSPACK* scaling algorithm. The FMM crystal structure was solved and refined using the *SHELX* program package (Sheldrick, 2015) and the *Olex2* software (Dolomanov, 2009).

Electron probe microanalyses (EPMA) of the NHMLA sample were performed at the University of Utah on a Cameca SX-50 electron microprobe with four wavelength dispersive spectrometers (WDS) and using *Probe for EPMA* package (Donovan *et al.*, 2012), at 15 kV accelerating voltage, 10 nA beam current and a beam diameter of 10 μm. Raw X-ray intensities were corrected for matrix effects with a φρ(z) algorithm (Pouchou and Pichoir, 1991). Standards used for EPMA are Cu metal for Cu, Zn metal for Zn, synthetic GaAs for As and apatite for P.

https://doi.org/10.1180/mgm.2022.36 Published online by Cambridge University Press

Table 1. Raman bands of holotype goldhillite and goldhillite, philipsburgite and kipushite by Ciesielczuk *et al.* (2016).

Range (cm^{-1})	This study	Ciesielczuk *et al.* (2016)			Tentative assignment
	Goldhillite As 1.63; P 0.37	Goldhillite As 1.63; P 0.39	Intermediate member* As 0.92; P 1.00	Kipushite As 0.70; P 1.21	
3600–3450	3546, 3489	3550, 3484	3549, 3484	3549, 3529 sh, 3482	O–H stretching vibrations of OH groups
3450–3100	3450–3100	3429, 3215	3442, 3295	3444, 3251	O–H stretching vibrations of H_2O molecules
1100–990	1051 sh	1060 sh, 994 sh	1065 sh, 1027 sh, 1001 sh	1078 sh, 1045 sh, 1021 sh	$\upsilon_3(PO_4)^{3-}$ and $(HOPO_3)^{2-}$ vibrations
990–900	969	970, 946 sh	972, 944 sh	975, 942 sh	υ_1 $(PO_4)^{3-}$ and $(HOPO_3)^{2-}$ stretching vibrations
900–850	860	878 sh, 865	867	875 sh, 869	$\upsilon_1(AsO_4)^{3-}$ and $(HOAsO_3)^{2-}$ stretching vibrations
850–750	833, 805, 784	847 sh, 809, 791 sh	837 sh, 813, 794 sh	843 sh, 814, 796 sh	$\upsilon_3(AsO_4)^{3-}$ and $(HOAsO_3)^{2-}$ stretching vibrations
750–600	–	667	671 sh	639 sh, 617 sh	Deformation modes within As···O–H group due to the delocalisation of the hydroxyl proton
600–420	560 sh, 525 sh, 497, 482 sh, 464 sh, 429 sh	564 sh, 491 sh, 474, 462 sh	564 sh, 483, 462 sh	552 sh, 493, 464 sh, 438	υ_4(O–As–O) modes
420–340	392, 370 sh, 359 sh	396, 368, 347 sh	401, 368, 347 sh	396, 369	υ_2(O–As–O) modes
330–90	325 sh, 308, 288, 241, 218 sh, 176, 157, 121, 96	317, 307, 249, 218 sh	314, 292, 249, 210 sh	317, 297, 256, 221 sh	Lattice modes

*Mineral with As:P ratio close to 1:1, probably philipsburgite. However it is not clear whether As and P are ordered or disordered in that species (Ciesielczuk *et al.*, 2016).

Table 2. Chemical data (in wt.%) for philipsburgite from the Black Pine mine (BP), Kamariza mines (KM) and Silver Coin mine (SC), and goldhillite from the Gold Hill mine (FMM) and Los Angeles Museum (NHMLA).

Constituent	BP*	KM (10 points on 3 crystals)		SC (19 points on 6 crystals)		FMM**	NHMLA (12 points on 6 crystals)	
	Mean	Mean	Range	Mean	Range	Mean	Mean	Range
ZnO	18.2	10.64	10.59–10.67	23.07	19.56–25.00	13.18	14.59	12.56–16.04
CuO	46.3	53.05	53.00–53.11	39.43	37.29–42.22	48.91	47.97	46.71–49.65
P_2O_5	8.7	5.61	5.55–5.70	9.80	8.58–10.56	3.25	2.63	2.26–3.15
As_2O_5	16.3	21.24	21.18–21.36	15.35	14.55–16.76	26.06	25.89	25.09–26.89
V_2O_5	n.d.	n.d.	n.d.	0.19	0.10–0.31	n.d.	n.d.	n.d.
H_2O	9.9	9.47§		10.62§		8.97§	9.38§	
Total	99.4	100.01		98.46		100.37	100.46	

* Peacor *et al.* (1987); ** Krivovichev *et al.* (2018); § Based on the structure
n.d. – not determined

Philipsburgite

Room-temperature single-crystal X-ray diffraction studies were done for the BP (holotype philipsburgite) and SC samples using a Rigaku R-Axis Rapid II curved imaging plate microdiffractometer. The data were collected using monochromatic Mo*K*α X-radiation at 50 kV and 40 mA. For the KM sample the measurement was done on a Bruker APEX II diffractometer equipped with a CCD area detector and an Incoatec Microfocus Source IμS (30 W, multilayer mirror and Mo*K*α).

Chemical analyses of the KM philipsburgite sample were done by means of a JEOL Hyperprobe JXA8530F with field-emission electron gun, operated in WDS mode at 10 kV accelerating voltage, 20 nA beam current and 30 μm beam diameter. Reference materials

https://doi.org/10.1180/mgm.2022.36 Published online by Cambridge University Press

Table 3. Data measurement and refinement information for philipsburgite crystals from the Black Pine mine (BP), Kamariza mines (KM) and Silver Coin mine (SC) and goldhillite crystal from Gold Hill mine (FMM).

	BP	KM	SC	FMM
Crystal Data				
*T*1 site occupancy*	$P_{0.879(6)}As_{0.121(6)}$	$P_{0.614(2)}As_{0.386(2)}$	$P_{0.850(5)}As_{0.150(5)}$	$As_{0.630(5)}P_{0.370(5)}$
*T*2 site occupancy*	$As_{0.898(6)}P_{0.102(6)}$	As	$As_{0.865(5)}P_{0.135(5)}$	As
Space group	$P2_1/c$	$P2_1/c$	$P2_1/c$	$P2_1/c$
a (Å)	12.3095(9)	12.3291(6)	12.3202(9)	12.3573(5)
b (Å)	9.2276(3)	9.2189(4)	9.2182(4)	9.2325(3)
c (Å)	10.7195(3)	10.7011(5)	10.7303(6)	10.7163(4)
β (°)	97.137(7)	97.249(2)	97.118(7)	97.346(4)
V (Å^3)	1208.16(10)	1206.57(2)	1209.24(12)	1212.59(8)
Z	4	4	4	4
ρ_{calc} (g cm^{-3})	4.056	4.151	4.048	4.188
μ (Mo*K*α) (mm^{-1})	13.57	14.56	13.52	15.10
Data collection and refinement				
Crystal size, mm	0.16 × 0.15 × 0.05	0.075 × 0.05 × 0.025	0.10 × 0.07 × 0.015	0.12 × 0.11 × 0.03
$2\theta_{max}$ (°)	54.86	80	50.05	62.152
Unique data (R_{int})	2729 (0.0900)	7613 (0.0589)	2126 (0.0741)	3358 (0.0589)
Data with $I_o > 2\sigma I$	2308	5485	1686	2365
Variables	234	235	234	228
R_1 [for $I_o > 2\sigma I$]	0.0521	0.0349	0.0386	0.0540
wR_2 [for all data]	0.1339	0.0688	0.0972	0.1077
Goodness-of-fit on F^2	1.086	1.029	1.088	0.999
$\Delta\rho_{min\ /\ max}$ (e^-Å^{-3})	−1.2 / 3.0	−1.4 / 1.2	−1.2 / 1.4	−1.3 / 1.7

* For all four refinements, all other sites were assigned full occupancies by their ideal constituents.

used for KM chemical analyses were zincite for Zn, cuprite for Cu, synthetic (OH)-apatite for P and arsenopyrite for As. EPMA for SC philipsburgite was done on a Cameca SX-50 operated in WDS mode at 15 kV accelerating voltage, 10 nA beam current and 10 μm beam diameter. Standards used were Cu metal for Cu, zincite for Zn, GaAs for As, apatite for P and V metal for V.

Table 4. Atom coordinates and equivalent isotropic displacement parameters (Å^2) and site occupancies (s.o.f.) for goldhillite (FMM).

Atom	Wyck.	*x*	*y*	*z*	U_{eq}	s.o.f
Cu1	4e	0.31916(8)	0.41696(10)	0.19179(8)	0.0123(2)	1
Cu2	4e	0.27985(9)	0.26495(11)	0.45252(8)	0.0140(2)	1
Cu3	4e	0.32305(8)	0.5857(1)	0.44691(8)	0.0102(2)	1
Cu4	4e	0.32329(8)	0.76275(10)	0.19492(8)	0.0103(2)	1
Cu5	4e	0.30857(8)	0.9317(1)	0.43606(8)	0.0104(2)	1
Zn1	4e	0.03377(8)	0.09381(12)	0.33286(9)	0.0216(3)	1
*T*1	4e	0.04315(9)	0.27434(14)	0.09864(10)	0.0195(4)	$As_{0.630(5)}$ $P_{0.370(5)}$
*T*2	4e	0.43052(7)	0.09175(8)	0.20385(6)	0.00848(18)	1
O_h1	4e	0.2424(4)	0.4361(6)	0.3413(4)	0.0110(11)	1
H_h1	4e	0.1683(11)	0.4530(30)	0.3250(20)	0.013	1
O2	4e	0.4349(4)	0.5834(6)	0.2904(4)	0.0098(11)	1
O_h3	4e	0.2492(5)	0.5893(6)	0.1012(4)	0.0124(12)	1
H_h3	4e	0.1742(12)	0.5930(20)	0.1130(40)	0.015	1
O_h4	4e	0.3757(4)	0.3969(6)	0.0292(4)	0.0100(11)	1
H_h4	4e	0.4330(40)	0.3300(70)	0.0280(60)	0.012	1
O5	4e	0.1636(5)	0.2123(7)	0.949(5)	0.0273(16)	1
O6	4e	0.3908(4)	0.2437(5)	0.2704(4)	0.0120(11)	1
O7	4e	0.3755(5)	0.4121(6)	0.5501(4)	0.0137(12)	1
O_h8	4e	0.1901(4)	0.1144(6)	0.3561(4)	0.0138(12)	1
H_h8	4e	0.2210(20)	0.0900(50)	0.2820(30)	0.017	1
O_h9	4e	0.2513(4)	0.7520(6)	0.3493(4)	0.0099(11)	1
H_h9	4e	0.1767(11)	0.7450(20)	0.3370(20)	0.012	1
O_h10	4e	0.4058(4)	0.7262(6)	0.5537(4)	0.0115(11)	1
H_h10	4e	0.4780(20)	0.7020(50)	0.5840(60)	0.014	1
O_W11	4e	0.1822(5)	0.5927(7)	0.5888(6)	0.0218(14)	1
H_W1A	4e	0.1140(40)	0.6410(90)	0.5720(70)	0.026	1
H_W1B	4e	0.1510(50)	0.5000(40)	0.5900(60)	0.026	1
O12	4e	0.3874(4)	−0.0535(6)	0.2828(4)	0.0108(11)	1
O13	4e	0.0545(6)	0.4275(9)	0.1723(8)	0.058(2)	1
O14	4e	−0.0232(5)	0.2956(8)	−0.0390(5)	0.0372(19)	1
O15	4e	−0.0302(6)	0.1696(9)	0.1707(5)	0.043(2)	1

Wyck. – Wyckoff positions

Results

Occurrence, general appearance and physical properties of goldhillite

The new mineral goldhillite occurs on surfaces of fractures in a rock comprised mostly of quartz with iron hydroxides. These surfaces are covered by a clay-like material on which the holotype goldhillite aggregates has grown in association with fine-grained aggregates and thin needles (up to 0.4 mm long) of a mixite-

Table 5. Selected bond lengths (Å) for goldhillite (FMM).

Cu1–O_h1	1.972(5)	Cu4–O2	2.309(5)	Zn–O_h8	1.925(5)
Cu1–O2	2.266(5)	Cu4–O_h3	2.044(5)	Zn–O13	1.880(7)
Cu1–O_h3	2.002(5)	Cu4–O_h9	1.978(4)	Zn–O14	1.916(6)
Cu1–O_h4	1.967(5)	Cu4–O_h10	1.933(5)	Zn–O15	1.946(6)
Cu1–O5	2.799(7)	Cu4–O_W11	2.367(6)	<Zn–O>	1.917
Cu1–O6	1.965(5)	Cu4–O12	2.050(5)		
<Cu1–O>	2.162	<Cu4–O>	2.114	*T*1–O5	1.600(6)
				*T*1–O13	1.617(8)
Cu2–O_h1	1.997(5)	Cu5–O_h3	2.009(5)	*T*1–O14	1.605(6)
Cu2–O_h4	2.016(6)	Cu5–O_h4	1.994(5)	*T*1–O15	1.591(7)
Cu2–O5	2.236(6)	Cu5–O_h8	2.325(6)	<*T*1–O>	1.603
Cu2–O6	2.532(5)	Cu5–O_h9	1.987(5)		
Cu2–O7	2.005(5)	Cu5–O_h10	2.499(5)	*T*2–O2	1.658(5)
Cu2–O_h8	1.984(5)	Cu5–O12	2.019(5)	*T*2–O6	1.675(5)
<Cu2–O>	2.128	<Cu5–O>	2.139	*T*2–O7	1.701(5)
				*T*2–O12	1.707 (5)
Cu3–O_h1	1.973(5)	O_h1–H_h1	0.923(13)	<*T*2–O>	1.685
Cu3–O2	2.305(5)	O_h3–H_h3	0.953(19)		
Cu3–O7	2.007(5)	O_h4–H_h4	0.94(2)		
Cu3–O_h9	2.000(5)	O_h9–H_h9	0.917(13)		
Cu3–O_h10	1.934(5)	O_h10–Hh10	0.93(2)		
Cu3–O_W11	2.454(6)	O_h8–H_h8	0.951(13)		
<Cu3–O>	2.112	O_W11–H_W1A	0.95(2)		
		O_W11–H_W1B	0.94(2)		

https://doi.org/10.1180/mgm.2022.36 Published online by Cambridge University Press

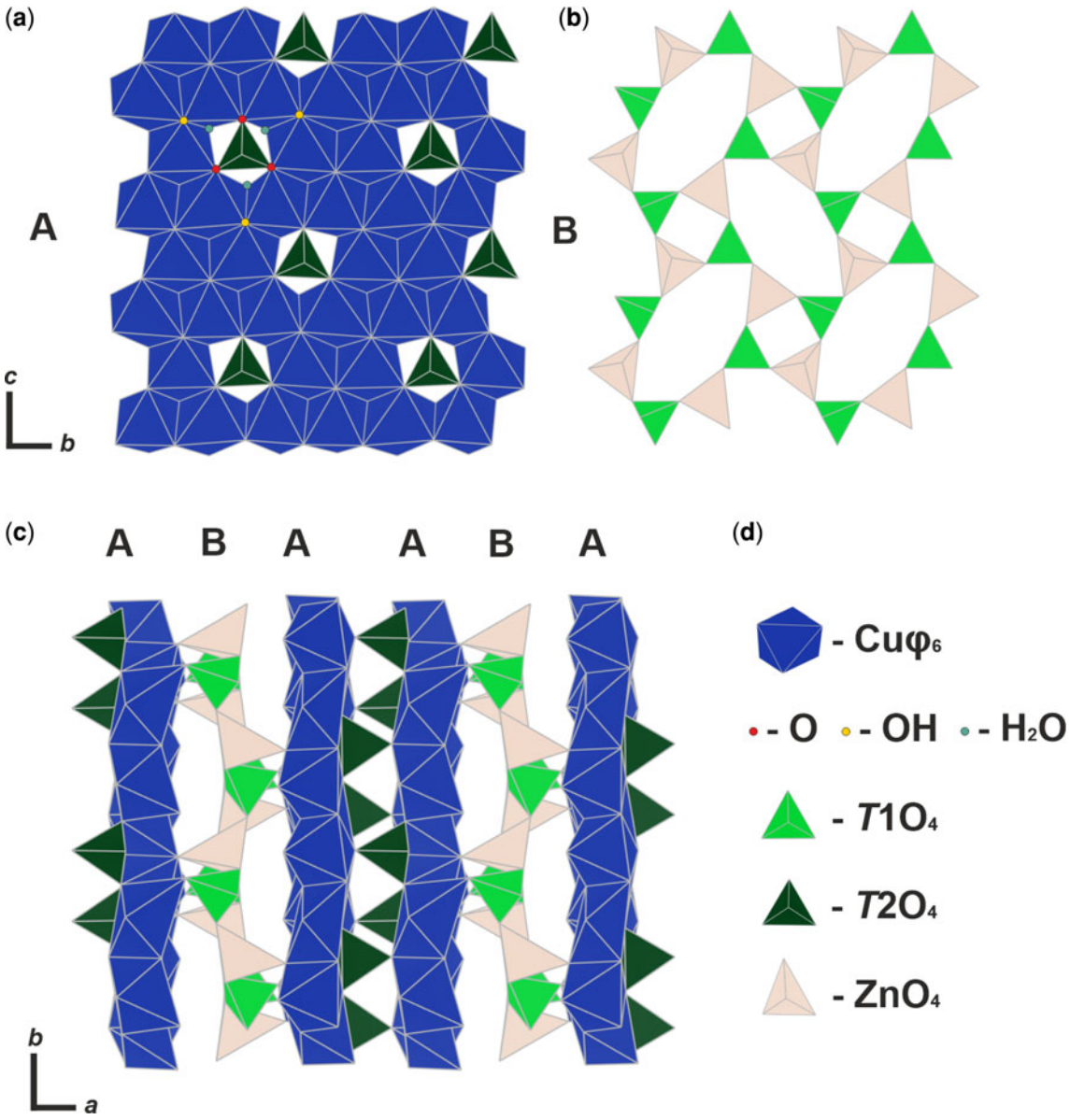

Fig. 5. The crystal structure of goldhillite: (a) the **A**-type layer; (b) the **B**-type layer; (c) crystal structure projected along the *c*-axis; and (d) legend, $\varphi = O^{2-}$, $(OH)^{-}$, H_2O; *T*1 and *T*2 are predominantly occupied by As.

group mineral, probably zálesíite (Fig. 1). On the cotype specimen, goldhillite has grown on botryoidal cornwallite coated with tiny crystals of conichalcite on garnet skarn matrix (Fig. 2). Previously, goldhillite from the Yamato mine (Yamaguchi Prefecture, Japan) was described as an As-dominant philipsburgite by Shirose and Uehara (2011); the mineral was found occurring in skarns within cavities of the oxidised rock in association with malachite, cornwallite, quartz and goethite. Goldhillite forms rosette-type aggregates (up to 1.5 mm in diameter) of subparallel to divergent tabular crystals, flattened on {100}, up to 1 mm across (Figs 2 and 3). The observed crystal forms are {100} (the major form), {110}, {001} and {111} (narrow lateral faces). Tablets are commonly curved. Twinning is not observed. The *a*:*b*:*c* ratio calculated from RT unit-cell parameters of the holotype is 1.3385:1:1.1607.

Goldhillite crystals are transparent, bright emerald green with vitreous lustre and pale green streak. Fluorescence is not observed. The mineral fracture is uneven; separate crystals are brittle. Perfect cleavage on {100} is observed. The hardness on the Mohs scale is 3.5, based on scratch tests. Goldhillite is readily soluble at room-temperature in diluted 10% HCl.

The optical properties were determined on cotype goldhillite using white light. Optically, goldhillite is biaxial (−) with $\alpha = 1.747(3)$, $\beta = 1.794(3)$ and $\gamma = 1.796(3)$. The 2V angle measured directly on a spindle stage is 17(3)°. The calculated 2V value is 22.8°. Dispersion is $r < v$, slight. The optical orientation is $Z = \mathbf{b}$, $X \wedge \mathbf{a} \approx 7°$ in the obtuse angle β. The pleochroism is X = light green, Y and Z = medium green; $X < Y \approx Z$.

The density could not be measured because of the paucity of available material and the unavailability of nearly concentrated Clerici solution. The density calculated on the basis of the empirical formula and unit-cell volume refined from single-crystal X-ray diffraction (XRD) data is 4.199 g/cm^{-3} for the holotype and 4.177 g/cm^{-3} for the cotype.

https://doi.org/10.1180/mgm.2022.36 Published online by Cambridge University Press

Table 6. Atom coordinates and equivalent isotropic displacement parameters (Å^2) and site occupancies (s.o.f.) for holotype philipsburgite (BP).

Atom	Wyck.	*x*	*y*	*z*	U_{eq}	s.o.f
Cu1	4e	0.32035(8)	0.41631(8)	0.19383(7)	0.0180(2)	1
Cu2	4e	0.27699(8)	0.26421(9)	0.45546(8)	0.0193(2)	1
Cu3	4e	0.32166(8)	0.58565(8)	0.44772(8)	0.0158(2)	1
Cu4	4e	0.32188(7)	0.76233(9)	0.19521(7)	0.0156(2)	1
Cu5	4e	0.030816(7)	0.93135(9)	0.43693(7)	0.0154(2)	1
Zn	4e	0.03303(7)	0.09466(8)	0.33443(8)	0.0189(2)	1
*T*1	4e	0.04368(13)	0.27599(16)	0.10043(14)	0.0177(5)	$P_{0.879(6)}$ $As_{0.121(6)}$
*T*2	4e	0.43058(6)	0.09035(7)	0.20432(6)	0.0119(3)	$As_{0.898(6)}$ $P_{0.102(6)}$
OH1	4e	0.2411(4)	0.4342(5)	0.3421(4)	0.0137(9)	1
H1	4e	0.167(2)	0.442(8)	0.307(6)	0.016	1
O2	4e	0.4339(4)	0.5818(5)	0.2907(5)	0.0170(10)	1
OH3	4e	0.2475(4)	0.5902(5)	0.1030(5)	0.0176(10)	1
H3	4e	0.173(2)	0.589(8)	0.068(7)	0.021	1
OH4	4e	0.3756(4)	0.3959(5)	0.0300(5)	0.0169(10)	1
H4	4e	0.4515(19)	0.383(8)	0.043(7)	0.020	1
O5	4e	0.1594(5)	0.2149(6)	0.0954(5)	0.0292(12)	1
O6	4e	0.3909(4)	0.2416(5)	0.2717(4)	0.0184(11)	1
O7	4e	0.3744(4)	0.4134(5)	0.5516(4)	0.0185(11)	1
OH8	4e	0.1915(4)	0.1093(5)	0.3580(4)	0.0177(10)	1
H8	4e	0.202(5)	0.116(6)	0.271(2)	0.021	1
OH9	4e	0.2488(4)	0.7520(5)	0.3500(4)	0.0168(10)	1
H9	4e	0.175(3)	0.758(8)	0.311(6)	0.020	1
OH10	4e	0.4051(4)	0.7266(5)	0.5524(5)	0.0186(10)	1
H10	4e	0.478(2)	0.703(5)	0.581(6)	0.022	1
OW11	4e	0.1793(5)	0.5916(5)	0.5897(5)	0.0250(12)	1
H11A	4e	0.111(3)	0.621(9)	0.550(7)	0.030	1
H11B	4e	0.162(5)	0.495(3)	0.609(7)	0.030	1
O12	4e	0.3878(4)	−0.0546(5)	0.2822(4)	0.0180(10)	1
O13	4e	0.0559(5)	0.4239(6)	0.1696(6)	0.0407(16)	1
O14	4e	−0.0205(5)	0.2939(6)	−0.0316(5)	0.0299(13)	1
O15	4e	−0.0258(4)	0.1733(6)	0.1720(4)	0.0271(12)	1

Wyck – Wyckoff position

Table 7. Selected bond lengths (Å) for philipsburgite (BP).

Cu1–O_h4	1.969(5)	Cu2–O_h8	1.992(5)	Cu3–O_h10	1.928(5)
Cu1–O6	1.968(5)	Cu2–O_h1	2.000(5)	Cu3–O_h1	1.985(5)
Cu1–O_h1	1.973(4)	Cu2–O_h4	2.014(5)	Cu3–O_h9	2.006(5)
Cu1–O_h3	2.028(5)	Cu2–O7	2.022(5)	Cu3–O7	2.002(5)
Cu1–O2	2.237(5)	Cu2–O5	2.219(5)	Cu3–O2	2.307(4)
Cu1–O5	2.824(6)	Cu2–O6	2.564(5)	Cu3–O_w11	2.460(6)
<Cu1–O>	2.166	<Cu2–O>	2.135	Cu3–O>	2.115
Cu4–O_h10	1.948(5)	Cu5–O_h9	1.993(5)	Zn1–O13	1.916(6)
Cu4–O_h9	1.986(5)	Cu5–O_h4	2.005(5)	Zn1–O_h8	1.940(5)
Cu4–O_h3	2.028(5)	Cu5–O_h3	2.024(5)	Zn1–O14	1.946(5)
Cu4–O12	2.048(5)	Cu5–O12	2.033(4)	Zn1–O15	1.942(5)
Cu4–O2	2.318(5)	Cu5–O_h8	2.275(5)	<Zn–O>	1.936
Cu4–O_w11	2.384(6)	Cu5–O_h10	2.481(5)		
<Cu4–O>	2.119	<Cu5–O>	2.135	O_h1–H1	0.94(2)
				O_h3–H3	0.95(2)
*T*1–O5	1.539(5)	*T*2–O2	1.664(5)	O_h4–H4	0.93(2)
*T*1–O14	1.542(6)	*T*2–O6	1.672(4)	O_h8–H8	0.96 (2)
*T*1–O15	1.543(6)	*T*2–O12	1.695(4)	O_h9–H9	0.95(2)
*T*1–O13	1.552(5)	*T*2–O7	1.696(5)	O_h10–H10	0.94(2)
<*T*1–O>	1.544	<*T*2–O>	1.682	O_w11–H_w1A	0.94(2)
				O_w11–H_w1B	0.95(2)

Raman spectroscopy of goldhillite

The Raman spectrum of goldhillite is shown in Fig. 4; the assignment of the bands is provided in Table 1. In general, the spectrum of goldhillite is in good agreement with those obtained for the minerals of the kipushite–philipsburgite series studied by Ciesielczuk *et al.* (2016). The stretching vibrations corresponding to hydroxyl ions are found around 3546 and 3489 cm^{-1}, whereas those corresponding to H_2O-molecules are seen as a wide band in the 3450–3100 cm^{-1} region. Several bands that can be assigned to arsenate anions occur in the 900–340 cm^{-1} region, whereas vibrations of phosphate anions have been observed in the region 1100–990 cm^{-1}. The bands in the region 330–90 cm^{-1} correspond to lattice vibrations. It should be noted that the Raman spectra reported by Ciesielczuk *et al.* (2016) for samples with different P/As ratios (corresponding to kipushite, intermediate member of the isomorphous series with As:P close to 1:1 and goldhillite) differ significantly in the relative intensities of phosphate (in particular, 975–970 cm^{-1}) and arsenate (in particular, 813–809 and 847–837 cm^{-1}) bands. Our sample shows a close resemblance to the As-dominant sample studied by Ciesielczuk *et al.* (2016).

Chemical data of goldhillite and philipsburgite

Goldhillite

Electron microprobe analyses were obtained for the determination of Cu, Zn, As and P. No other elements were detected. The H_2O content was calculated based upon the structure determination (Cu + Zn + As + P = 8 for goldhillite, O = 15 apfu). There was no damage caused by the electron beam.

Analytical data for the crystals of NHMLA goldhillite are given in Table 2 along with the data reported by Krivovichev *et al.* (2018) for the holotype FMM specimen.

The empirical formula for cotype goldhillite (NHMLA) based on O = 15 apfu is $(Cu_{4.62}Zn_{1.37})_{\Sigma 5.99}[(As_{0.86}P_{0.14})_{\Sigma 1.00}O_4]_2(OH)_6{\cdot}H_2O$ (–0.02 H for charge balance); this is in good agreement with the empirical formula reported by Krivovichev *et al.* (2018) for holotype goldhillite (FMM), $(Cu_{4.69}Zn_{1.23})_{\Sigma 5.92}(As_{0.86}P_{0.18}O_4)_2(OH)_{5.61}{\cdot}H_2O$. The ideal formula of goldhillite is $Cu_5Zn(AsO_4)_2(OH)_6{\cdot}H_2O$, which requires CuO 50.92, ZnO 10.42, As_2O_5 29.43, H_2O 9.23, total 100 wt.%.

Philipsburgite

Electron microprobe analyses of philipsburgite were obtained for the determination of Cu, Zn, As, P (for KM, SC and BP) and V (for SC). No further elements were detected. The H_2O content was calculated based upon the structure determination (P + As + V = 2 and O = 15 apfu).

Analytical data for the KM and SC samples are given in Table 2 along with the EPMA reported by Peacor *et al.* (1985) for the holotype BP sample. Table 2 provides a comparison of chemical data for goldhillite and philipsburgite.

The empirical formulas calculated on the basis of P + As + V = 2 and O = 15 apfu are $(Cu_{5.05}Zn_{0.99})_{\Sigma 6.04}[(AsO_4)_{1.40}(PO_4)_{0.60}]_{\Sigma 2}(OH)_6{\cdot}H_2O$ for the KM sample and $(Cu_{3.62}Zn_{2.07})_{\Sigma 5.69}[(AsO_4)_{0.976}(PO_4)_{1.009}(VO_4)_{0.015}]_{\Sigma 2}(OH)_6{\cdot}H_2O$ (+0.61 H for charge balance) for SC; that reported by Peacor *et al.* (1985) for holotype philipsburgite (BP) is $(Cu_{4.30}Zn_{1.65})_{\Sigma 5.95}[(AsO_4)_{1.05}(PO_4)_{0.91}](OH)_{6.03}{\cdot}1.04H_2O$. Although these formulas show significant variability in Cu *vs* Zn and As *vs* P, the results of the structure refinements (see below) are all consistent with the simplified formula $Zn(Cu,Zn)_5[(As,P)O_4][(P,As)O_4](OH)_6{\cdot}H_2O$ and with the ideal formula $Cu_5Zn(AsO_4)(PO_4)(OH)_6{\cdot}H_2O$, which requires 53.96 CuO, 11.04 ZnO, 15.59 As_2O_5, 9.63 P_2O_5, 9.78 H_2O, total 100 wt.%.

https://doi.org/10.1180/mgm.2022.36 Published online by Cambridge University Press

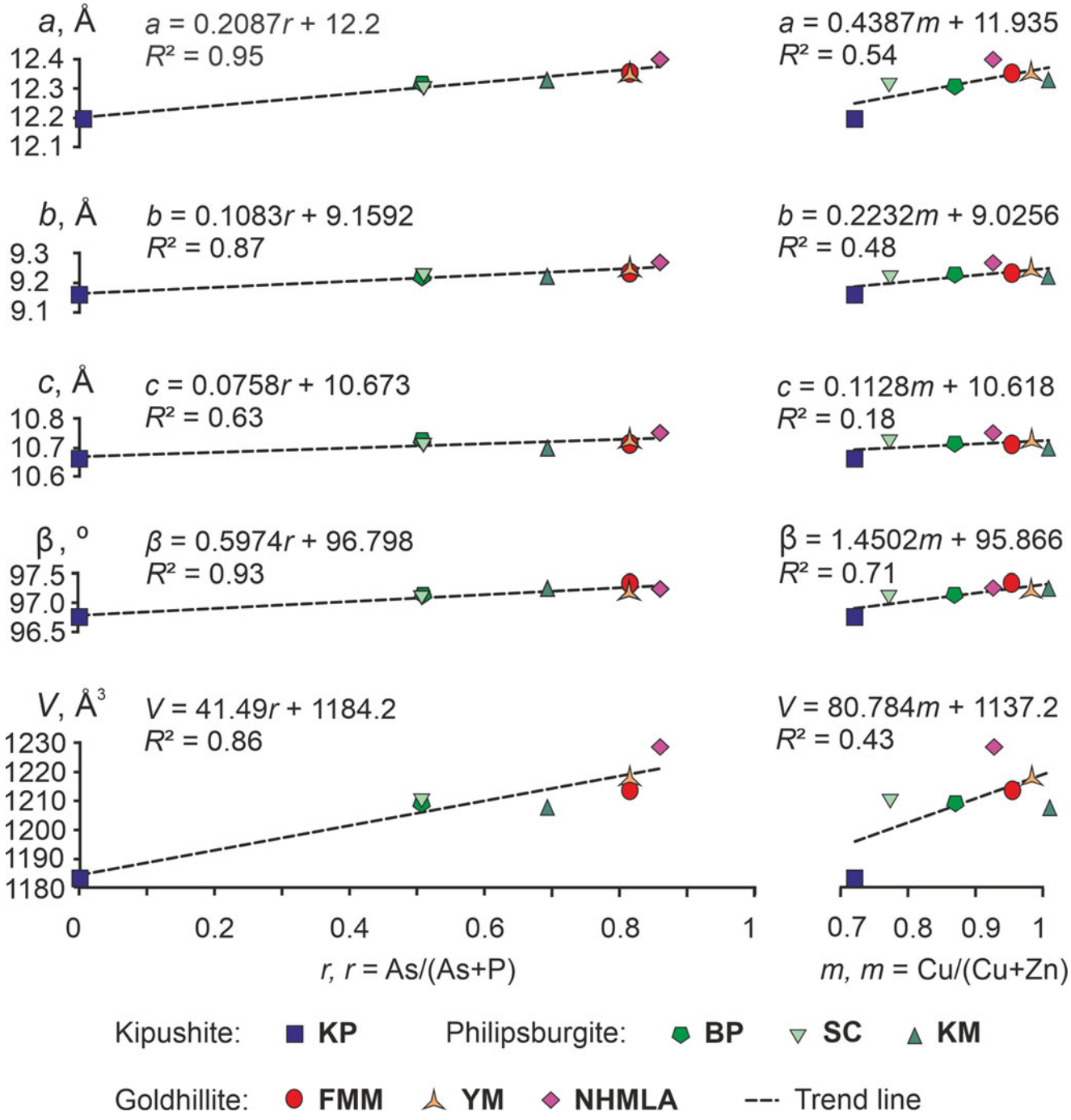

Fig. 6. The dependences of unit cell parameters of kipushite (KP) from Kipushi mine, Zaire (Piret *et al.*, 1985), philipsburgite (BP, SC, KM) and goldhillite (FMM, NHMLA, YM), where YM = the sample of goldhillite from Yamato mine, Yamaguchi Prefecture, Japan (Shirose and Uehara, 2011), versus tetrahedral As/(As + P) (*r*) and octahedral Cu/(Cu + Zn) values (m).

X-ray diffraction and crystal structure

Goldhillite

Powder X-ray diffraction data for holotype goldhillite are provided in Supplementary Table S1. The powder XRD pattern of goldhillite is in good agreement with the data reported for philipsburgite (ICDD 00-038-0384)* and the calculated pattern of kipushite (ICDD 01-084-0926). Goldhillite is monoclinic, $P2_1/c$ (#14), $a = 12.3808(4)$, $b = 9.2397(5)$, $c = 10.7862(5)$ Å, $\beta = 97.536(2)°$, $V = 1223.24(9)$ Å^3 and $Z = 4$.

The crystal structure of the holotype (FMM) sample was solved and refined to $R_1 = 0.054$ for 2365 independent reflections with $I > 2\sigma(I)$. The goldhillite structure was refined in space group $P2_1/c$ (#14) with the following unit-cell parameters: $a = 12.3573(5)$, $b = 9.2325(3)$, $c = 10.7163(4)$ Å, $\beta = 97.346(4)°$, $V = 1212.59(8)$ Å^3 and $Z = 4$. The crystallographic information file of the FMM sample is deposited at CCDC/FIZ Karlsruhe

*ICDD – International Centre for Diffraction Data, https://www.icdd.comICDD

https://doi.org/10.1180/mgm.2022.36 Published online by Cambridge University Press

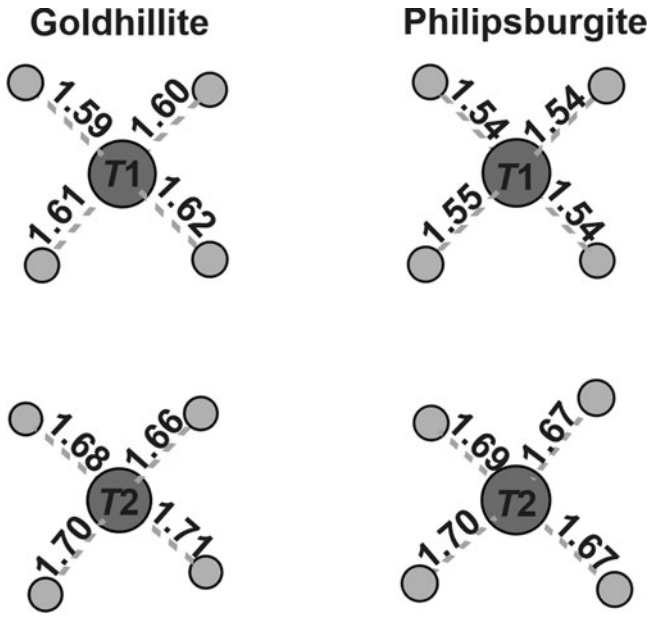

Fig. 7. The bond lengths (Å) of $T1O_4$ and $T2O_4$ tetrahedra of goldhillite (FMM) and philipsburgite (BP). Average values for goldhillite are < *T*1–O> ≈ 1.605 Å, <*T*2–O> ≈ 1.6875 Å; and for philipsburgite are < *T*1–O> ≈ 1.5425 Å and < *T*2–O> ≈ 1.685 Å.

database under the CSD number 2111718 [https://www.ccdc.cam.ac.uk/structures/] and as Supplementary material (see below).

The crystal-structure data for the cotype (NHMLA) sample were refined to $R_1 = 0.043$ for 2323 independent reflections with $I > 2\sigma(I)$ and unit-cell parameters: $a = 12.4040(9)$, $b = 9.2692(4)$, $c = 10.7585(5)$ Å, $\beta = 97.255(7)°$, $V = 1227.06(12)$ Å^3 and $Z = 4$. The obtained structure refinement for the NHMLA sample is completely consistent with that for the FMM sample, consequently, only the FMM structure is reported.

Details for the single-crystal X-ray data collection and structure refinement are provided in Table 3. Atom coordinates, site occupancies and isotropic displacement parameters are given in Table 4; anisotropic displacement parameters are listed in Supplementary Table S2. Selected bond lengths are given in Table 5.

The crystal structure of goldhillite, isotypic to those of philipsburgite and kipushite (Piret *et al.*, 1985), is shown in Fig. 5. It consists of five independent Cu sites, each surrounded by six ligands forming Jahn–Teller-distorted $Cu\varphi_6$ octahedra [$\varphi = O^{2-}$, $(OH)^-$, H_2O], one Zn site and two As sites (*T*1 and *T*2) in tetrahedral coordination. The $Cu\varphi_6$ octahedra share edges to form honeycomb-like layers (referred to as **A**-type) with open hexagonal holes covered by the $T2O_4$ tetrahedra (Fig. 5a). Alternating corner-sharing ZnO_4 and $T1O_4$ tetrahedra form four- and eight-membered tetrahedral rings in a second type of layer (referred to as **B**-type) (Fig. 5b). The **A**- and **B**-type layers are stacked perpendicular to the *a*-axis with adjacent A-type layers linking through their $T2O_4$ tetrahedra to form double-**A** layers. Single B-type layers link double-**A** layers, providing an overall **A**:**B** ratio of 2:1 (Fig. 5c).

The arrangement of the O-atoms, OH-groups and H_2O-molecules in the octahedral layer was determined from the analysis of bond-valence sums (BVS) incident upon the O sites. There are three types of O atoms in the layer (Fig. 5a). Atoms of type 1 are shared between $Cu\varphi_6$ octahedra and $T1O_4$ or $T2O_4$ tetrahedra, receiving BVS close to 2 valence units (vu); these are the O atoms. Atoms of type 2 are corner-shared between three $Cu\varphi_6$ octahedra, receiving BVS close to 1 vu and therefore are considered as the OH-groups. Atoms of type 3 are corner-shared between two $Cu\varphi_6$ octahedra; their BVS are <0.67 vu; these atoms are considered as the O atoms of the H_2O-molecules. The O–H bonds of the OH- and H_2O-groups point in the direction of the tetrahedral layer. The detailed description of the hydrogen-bonding scheme was reported by Krivovichev *et al.* (2018) for the sample studied at 100 K.

Philipsburgite

The crystal structure of philipsburgite was solved and refined at room temperature to $R_1 = 0.052$ (BP), 0.03 (KM) and 0.04 (SC) for 2308, 5485, 1686 independent reflections with $I > 2\sigma(I)$, respectively.

Details for the data collections and structure refinements are given in Table 3. Atom coordinates, site occupancies and isotropic displacement parameters are listed in Table 6 (BP), Supplementary Table S3 (KM), Table S4 (SC). Anisotropic displacement parameters

Table 8. Comparison of goldhillite, philipsburgite and kipushite.

Mineral	Goldhillite	Philipsburgite	Kipushite
Crystal chemical formula	$Cu_5Zn(AsO_4)_2(OH)_6{\cdot}H_2O$	$Cu_5Zn(AsO_4)(PO_4)(OH)_6{\cdot}H_2O$	$Cu_5Zn(PO_4)_2(OH)_6{\cdot}H_2O$
Symmetry	Monoclinic	Monoclinic	Monoclinic
Space group	$P2_1/c$	$P2_1/c$	$P2_1/c$
a, Å	12.3573(5)	12.3291(6)	12.197(2)
b, Å	9.2325(3)	9.2189(4)	9.156(2)
c, Å	10.7163(4)	10.7011(5)	10.667(2)
β, °	97.346(4)	97.249(35)	96.77(2)
V, Å^3	1212.59(8)	1206.57	1182.939
ρ_{calc} (g cm^{-3})	4.188	4.040	3.904
The strongest lines in the powder XRD pattern: [*d*, Å (*I*, %)]	4.09 (28), 3.41 (23), 2.57 (100), 2.17 (18), 1.95 (22), 1.54 (20)	12.2 (80), 4.05 (90), 3.405 (50), 2.666 (60), 2.559 (100), 1.534 (60)	12.2 (50), 4.03 (100), 3.386 (50), 2.970 (60), 2.554 (90), 1.531 (60)
Optical properties	Biaxial (–). Pleochroism: *X* light green, *Y* and *Z* medium green.	Biaxial (–). Pleochroism: *X* pale green, *Y* and *Z* medium green.	Biaxial (–). Pleochroism: *X* colourless, *Y* blue, *Z* bright blue.
	α = 1.747(3)	α = 1.729(2)	α = 1.693(2)
	β = 1.794(3)	β = 1.774(2)	β = 1.738(2)
	γ = 1.796(3)	γ = 1.775(2)	γ = 1.740(2)
	$2V_{meas}$ = 17(3)°	$2V_{meas}$ = 16(2)°	$2V_{calc}$ = 23°
Reference	This study	Peacor *et al.* (1985)	Piret *et al.* (1985)

https://doi.org/10.1180/mgm.2022.36 Published online by Cambridge University Press

are provided in Table S5 (BP), Table S6 (KM) and Table S7 (SC). Bond lengths are given in Table 7 (BP), Table S8 (KM) and Table S9 (SC). Crystallographic information files for the BP, SC and KM samples are deposited at CCDC/FIZ Karlsruhe database under the CSD numbers 2111715, 2111716 and 2111717, respectively [https://www.ccdc.cam.ac.uk/structures/], and as supplementary material.

Philipsburgite is isotypic with goldhillite and kipushite. The **B**-type layer of philipsburgite is constructed from corner-sharing ZnO_4 and $T1O_4$ tetrahedra with $T1$ predominantly occupied by P in contrast to goldhillite, where As predominates at both $T1$ and $T2$ sites and kipushite, which is P-dominant at both $T1$ and $T2$ sites.

Discussion

Philipsburgite, originally defined as the As end-member of a series with kipushite, is redefined herein as the As–P ordered intermediate species, with the formula $Cu_5Zn(AsO_4)(PO_4)(OH)_6{\cdot}H_2O$. Goldhillite is described as the As end-member with the formula $Cu_5Zn(AsO_4)_2(OH)_6{\cdot}H_2O$ [or $Cu_5Zn(AsO_4)(AsO_4)(OH)_6{\cdot}H_2O$]. Kipushite, $(Cu,Zn)_5Zn(PO_4)_2(OH)_6{\cdot}H_2O$ [or $Cu_5Zn(PO_4)(PO_4)(OH)_6{\cdot}H_2O$] is the P-dominant analogue of philipsburgite and its status as a mineral species remains unchanged. The difference between the mineral species forming this isomorphous series is the occupancy of two symmetrically independent tetrahedral sites, $T1$ and $T2$. Previous studies have shown that both As and P can occupy these sites with P preferring $T1$, and As preferring $T2$. Thus, the whole isomorphic series can be described as goldhillite (As >> P with As > 50% in both $T1$ and $T2$ sites) – philipsburgite (As ≈ P with As > 50% in the $T2$ site (or alternatively in the $T1$ site) and P > 50% in the $T1$ site (or alternatively in the $T2$ site)) – kipushite (P >> As with P > 50% in the $T1$ and $T2$ sites). The three minerals are isotypic and crystallise in the monoclinic $P2_1/c$ space group. The minerals of the isomorphous series can be distinguished from each other using the As:P ratio determined from quantitative chemical analyses with P:As > 3:1 identified as kipushite, and those with As:P > 3:1 identified as goldhillite and those with P ≈ As qualified as philipsburgite. Phases having P:As ratio outside the indicated ranges can be identified by checking if P and As are ordered in the $T1$ and $T2$ sites.

The substitution of P by As in the tetrahedral sites results in an increase of the unit-cell parameters due to the larger ionic radius of As compared to that of P. Such a dependence has been demonstrated by Shirose and Uehara (2011). In this work, we provide an updated correlation between the As/(As + P) or Cu/(Cu + Zn) (for octahedral Cu-positions) ratios and the unit-cell parameters (Fig. 6). The data show a linear correlation between the As/(As + P) ratio and the unit-cell parameters (with a goodness-of-fit, R^2, ranging from 0.63 to 0.95). The dependence of Cu/(Cu + Zn) ratio versus unit-cell parameters is less obvious, it shows a linear correlation for the a, b unit-cell parameters and the β angle (with R^2 ranging from 0.48 to 0.71) and an absence of a correlation for the c parameter ($R^2 = 0.18$). Probably, the Cu/(Cu + Zn) ratio contributes to the value of the unit-cell parameters, though not as significantly as the As/(As + P) ratio. The As:P ratio can also be inferred from the occupancies of the T sites and the $T1$–O and $T2$–O bond lengths, which are in the ranges 1.52–1.56 Å for kipushite (Piret *et al.*, 1985), 1.54–1.70 Å for philipsburgite and 1.59–1.71 Å for goldhillite (Fig. 7). Therefore, the unit-cell parameters increase along the sequence kipushite => philipsburgite => goldhillite; the same trend is noted for density, which is equal to 3.904, 4.040 and 4.199 g cm^{-3}, respectively (Table 8). Thus, although minerals of the isomorphous series are isotypic and have similar powder X-ray diffraction patterns, they can be distinguished by their unit-cell parameters using the equations presented in Fig. 6.

All three minerals, goldhillite, philipsburgite and kipushite, exhibit the same crystal morphology and form transparent bright emerald-green tabular crystals with vitreous lustre. Goldhillite, philipsburgite and kipushite are biaxial (–), and possess distinct pleochroism. The pleochroism of goldhillite is light green along the X axis, and medium green along both Y and Z axes. The pleochroism of philipsburgite is pale green along the X axis, and medium green along the Y and Z axes (Peacor *et al.*, 1985). The pleochroism of kipushite is colourless along the X axis, blue along the Y axis and bright blue along the Z axis (Piret *et al.*, 1985). The values of the refraction indices increase in the sequence kipushite => philipsburgite => goldhillite (Table 8). Thus, the minerals of the goldhillite–philipsburgite–kipushite isomorphous series can also be discriminated by their optical properties.

The Raman spectrum of goldhillite differs significantly from those of philipsburgite and kipushite by the strong bands of arsenate ions (in particular, 813–809 and 847–837 cm^{-1}) and the weak bands of phosphate ions (in particular, 975–970 cm^{-1}) (Table 1, Fig. 4).

Thus, the goldhillite–philipsburgite–kipushite isomorphic series includes three mineral species: the As-dominant member (goldhillite, the new mineral, defined herein), an As–P ordered member (philipsburgite, redefined herein) and a P-dominant member (kipushite).

Acknowledgements. This work was supported by the Russian Foundation for Basic Research, project number 20-35-90007 (for FMM sample research) as well as by University Vienna grants IS526001 and IP532010 (the KM sample). The investigations were carried out using the equipment of the Geomodel and X-ray Diffraction Centres of Saint-Petersburg State University. Studies conducted at the Natural History Museum of Los Angeles County were supported by the John Jago Trelawney Endowment. We thank Structural Editor Peter Leverett and four anonymous reviewers for their critical comments and the journal Editors for the manuscript handling.

Supplementary material. To view supplementary material for this article, please visit https://doi.org/10.1180/mgm.2022.36

Competing interests. The authors declare none

References

Agilent Technologies (2014) *CrysAlisPro Software system, version 1.171.37.35*. Agilent Technologies UK Ltd, Oxford, UK.

Britvin S.N., Dolivo-Dobrovolsky D.V. and Krzhizhanovskaya, M.G. (2017) Software for processing of X-ray powder diffraction data obtained from the curved image plate detector of Rigaku RAXIS Rapid II diffractometer. *Zapiski Rossiiskogo Mineralogicheskogo Obshchetstva*, **146**, 104–107.

Bruker-AXS (2009) *TOPAS V4.2: General Profile and Structure Analysis Software for Powder Diffraction Data*. Karlsruhe, Germany.

Ciesielczuk J., Janeczek J., Dulski M. and Krzykawski T. (2016) Pseudomalachite–cornwallite and kipushite–philipsburgite solid solutions: chemical composition and Raman spectroscopy. *European Journal of Mineralogy*, **28**, 555–569.

Dolomanov O.V., Bourhis L.J., Gildea R.J., Howard J.A.K. and Puschmann H. (2009) OLEX2: a complete structure solution, refinement and analysis program. *Journal of Applied Crystallography*, **42**, 339–341.

Donovan J., Kremser D. and Fournelle J. (2012) *Probe for EPMA: acquisition, automation and analysis*. Probe Software, Inc., Eugene, Oegon, USA.

Horiba Jobin Vyon (2008) *LabSpec software 5.54.15*. Horiba, Jobin Vyon, Japan.

Ismagilova R.M., Kampf A.R., Zhitova E.S., Zolotarev A.A., Ciesielczuk J., Mikhailova J.A., Belakovsky D.I., Bocharov V.N., Shilovskikh V.V., Vlasenko N.S., Nash B.P. and Krivovichev S.V. (2021) Goldhillite, IMA 2021-034. CNMNC Newsletter 62. *Mineralogical Magazine*, **85**, 634–638, https://doi.org/10.1180/mgm.2021.62

Krivovichev S.V., Zhitova E.S., Ismagilova R.M. and Zolotarev A.A. (2018) Site-selective As–P substitution and hydrogen bonding in the crystal structure of philipsburgite, $Cu_5Zn((As,P)O_4)_2(OH)_6{\cdot}H_2O$. *Physics and Chemistry of Minerals*, **45**, 917–923.

Miyawaki R., Hatert F., Pasero M. and Mills S. (2021). Newsletter 60. *Mineralogical Magazine*, **85**, 454–458, doi:10.1180/mgm.2021.30

Olmi F., Sabelli C. and Brizzi G. (1988) Agardite-(Y), Gysinite-(Nd) and other rare minerals from Sardinia. *The Mineralogical Record*, **19**, 305–310.

OriginLab Corporation (2009) *OriginLab 8.1*. Northampton, Massachusetts, USA.

Peacor D., Dunn P.J., Ramik R., Sturman B. and Zeihen L. (1985) Philipsburgite, a new copper zinc arsenate hydrate related to kipushite, from Montana. *The Canadian Mineralogist*, **23**, 255–258.

Piret P., Deliens M. and Piret-Meunier J. (1985) Occurrence and crystal structure of kipushite, a new copper-zinc phosphate from Kipushi, Zaire. *The Canadian Mineralogist*, **23**, 35–42.

Pouchou J.L. and Pichoir F. (1991) Quantitative analysis of homogeneous or stratified microvolumes applying the model "PAP". Pp. 31–76 in: *Electron Probe Quantitation* (Heinrich K. and Newbury D., editors). Plenum Press, New York, https://doi.org/10.1007/978-1-4899-2617-3_4.

Sheldrick G.M. (2015) Crystal structure refinement with SHELXL. *Acta Crystallographica*, **A71**, 3–8.

Shirose Y. and Uehara S. (2011). Philipsburgite from the Yamato mine, Yamaguchi Prefecture, Japan. *Journal of Mineralogical and Petrological Sciences*, **106**, 153–157. http://doi.org/10.2465/jmps.101021e

Siidra O.I., Nazarchuk E.V., Pautov L.A., Borisov A.S. and Kozin M.S. (2021) Milkovoite, IMA 2021-005. CNMNC Newsletter 61; *Mineralogical Magazine*, **85**, https://doi.org/10.1180/mgm.2021.48

Yakovenchuk V.N., Pakhomovsky Y.A., Konoplyova N.G., Panikorovskii T.L., Mikhailova Y.A, Bocharov V.N, Krivovichev S.V and Ivanyuk G.Y. (2017) Epifanovite $NaCaCu_5(PO_4)_4[AsO_2(OH)_2]{\cdot}7H_2O$, a new mineral from the Kester deposit (Sakha-Yakutia, Russia). *Zapiski Rossiiskogo Mineralogicheskogo Obshchetstva*, **146**, 30–39 [in Russian].

https://doi.org/10.1180/mgm.2022.36 Published online by Cambridge University Press